Hearing Research 462 (2025) 109288

Contents lists available at ScienceDirect

Hearing Research

journal homepage: www.elsevier.com/locate/heares

Toward an *ex vivo* preparation for studies of the cochlear active process in mammals

Francesco Gianoli [1,*], Rodrigo Alonso [1], Brian Fabella, A.J. Hudspeth

Howard Hughes Medical Institute and Laboratory of Sensory Neuroscience, The Rockefeller University, 1230 York Avenue, NY, NY 10065, USA

ARTICLE INFO

Keywords:
Active process
Cochlea
Cochlear amplifier
Cochlear mechanics
Cochlear microphonics
Compressive nonlinearity
Dynamical systems
Endocochlear potential
Ex vivo preparation
Hair cell physiology
Hopf bifurcation
Mammalian hearing
Microphonic potential
Mongolian gerbil
Organ of Corti
Transepithelial pressure

ABSTRACT

The mammalian cochlea benefits from an active process characterized by amplification of mechanical inputs, sharp frequency selectivity, compressive nonlinearity, and spontaneous otoacoustic emission. Similar traits are observed in individual hair cells of nonmammalian tetrapods, in which they emerge from the critical dynamical regime of hair cells operating near a Hopf bifurcation. It remains unclear whether a similar critical regime also underpins the active process of the mammalian cochlea. Efforts to address this question have been limited in part by the absence of an *ex vivo* preparation that both preserves the physiological integrity of the sensory epithelium and grants direct experimental access to it. To overcome these problems, we improved a two-compartment cochlear preparation (Chan and Hudspeth, 2005a, 2005b) to more closely simulate *in vivo* conditions and used it to conduct electrophysiological recordings of microphonic signals in isolated cochlear segments of the Mongolian gerbil. Our methodological advances included refining the dissection protocol to reduce the size of the exposed cochlear segment and altering the ionic compositions of the solutions to better control the Ca^{2+} concentration. We also maintained a constant temperature in order to stabilize the experimental conditions. Most critically, by introducing a mechanism to adjust the pressure in the endolymphatic compartment, we were able to explore how variations in transepithelial pressure influence the electrical response. These changes enabled us to reliably measure compressive nonlinearities with a one-third power law similar to that observed from cochleas *in vivo* and consistent with the behavior of a dynamical system operating near a Hopf bifurcation.

1. Introduction

The ear's active process optimizes responsiveness to sound through three defining characteristics: it expends energy to amplify stimuli, sharpens frequency selectivity, and demonstrates compressive nonlinearity (Hudspeth, 2008, 2014). The system condenses a broad intensity range of input signals into a narrow output range and thereby increases the ear's sensitivity to softer sounds while preventing damage from louder ones. Although disruption of the active process causes hearing loss, the mechanism by which it operates remains unclear.

The active process originates from the activity of hair cells, the sensory receptors of the ear. These cells act as microphones, for they detect sound vibrations with their mechanosensitive structures, and they serve as amplifiers that enhance the stimuli that they receive. Their operation relies on molecular springs, the tip links, that connect to mechanically sensitive ion channels that open and close in unison with periodic stimuli (Pickles, 2012). These hair cells are located in the organ of Corti, an intricate sensory epithelium situated between the tectorial and basilar membranes and stretching along the entire cochlear spiral. The somata of the hair cells, which are interspersed among supporting cells in the organ of Corti, are positioned atop the basilar membrane and in contact on their basolateral surfaces with an extracellular fluid called *perilymph*. The cells' sensory microvilli—grouped into hair bundles—extend into a chamber filled with a Na^{+}-poor solution called *endolymph*, with the gel-like tectorial membrane resting upon them.

When sound-driven vibrations reach the cochlea, they generate a traveling wave that progresses along the basilar membrane from the cochlea's base toward its apex. This wave peaks at a specific location along the cochlear spiral that depends on the frequency of the sound. High frequencies evoke the greatest movement in the basal portion of the organ of Corti, whereas lower frequencies propagate further along the spiral to activate more apical areas. The high sensitivity of hearing results from the synergy between the traveling wave and active movements produced by the hair cells within the organ of Corti.

* Corresponding author.
E-mail address: fgianoli@rockefeller.edu (F. Gianoli).
[1] These authors contributed equally to the work.

https://doi.org/10.1016/j.heares.2025.109288
Received 30 November 2024; Received in revised form 18 April 2025; Accepted 22 April 2025
Available online 24 April 2025
0378-5955/© 2025 The Authors. Published by Elsevier B.V. This is an open access article under the CC BY license (http://creativecommons.org/licenses/by/4.0/).

Two principal theories have been proposed to account for the active process in mammals: membrane-based somatic electromotility and active hair-bundle motility. The first involves a strictly mammalian type of hair cell, the outer hair cell, which is capable of changing its length in response to changes in the membrane potential (Ashmore, 1987; Dallos, 2008). The latter mechanism, which has been demonstrated in non-mammalian vertebrates, involves the hair bundle's capacity to exert forces that amplify mechanical stimuli (Martin and Hudspeth, 1999). Together with a Ca^{2+}-dependent adaptation mechanism, myosin motors located at the upper end of the tip links situate the system near a dynamical instability known as a Hopf bifurcation (Hudspeth et al., 2010; Hudspeth and Martin, 2024).

A bifurcation represents a situation in which, for whatever reason, a dynamical system is poised such that a minuscule change in some characteristic of the system—the so-called control parameter—strikingly alters the system's behavior (Strogatz, 1994). A critical regime of this sort is important in that it might manifest properties that are not characteristic of either of the adjacent regimes (Hudspeth and Martin, 2024). At a Hopf bifurcation in particular, a system's sensitivity to inputs grows enormously. The system can discriminate highly between stimuli of different frequencies. And the system's response near the bifurcation is expected to grow as the cube root of an increasing stimulus, and thus to exhibit compressive nonlinearity (Martin and Hudspeth, 1999). All these properties are attractive features for an auditory system, and they might well coincide with the observation that a mammalian cochlea exhibits amplification, frequency tuning, and compressive nonlinearity (Hudspeth et al., 2010).

The exact mechanism by which individual hair cells contribute to the active process observed in the cochlea remains elusive. This problem stems in part from the challenging nature of studying hair cells *ex vivo*. Encased within the dense temporal bone, the cochlea poses a formidable barrier to direct examination, and dissection typically leads to

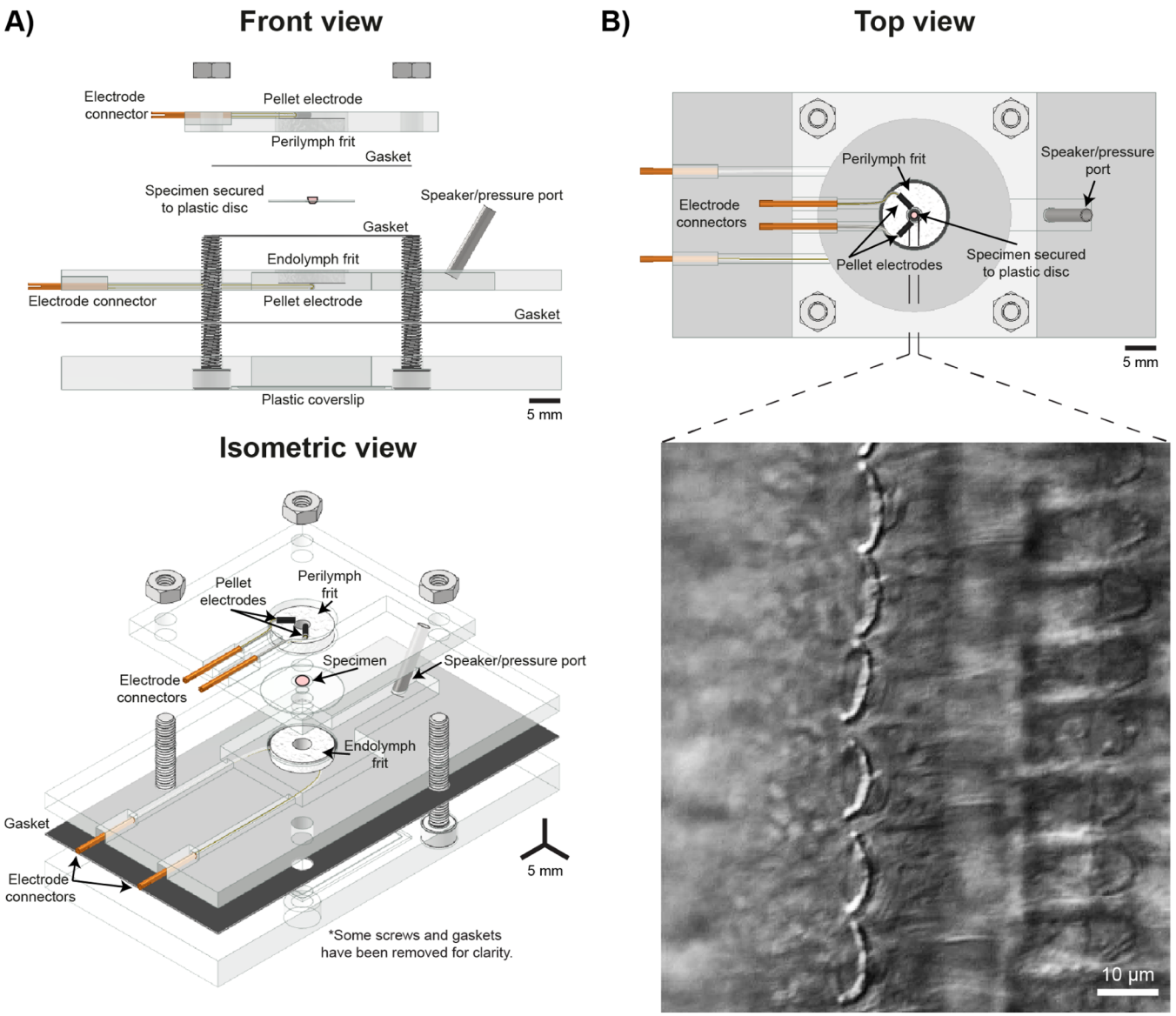

Fig. 1. Schematic diagram of the two-compartment acrylic chamber. (A) As shown in the front and isometric views, the various components are stacked and then clamped together using bolts and nuts. The specimen secured to the plastic disc is placed between two glass frits. A frit wetted with perilymph and a frit wetted with endolymph ensure that the basal and apical surfaces of the cochlear segment are continuously exposed to the appropriate physiological solutions. Silicone-rubber gaskets maintain a tight seal between the two compartments. Pairs of Ag/AgCl pellet electrodes are used to impose an endocochlear potential and to measure the cochlear microphonic potential across the sensory epithelium. Acoustic stimuli and pressure are delivered and controlled through the speaker-pressure port to the lower compartment. (B) A top view provides another perspective of the experimental chamber. The inset shows a row of inner hair cell bundles as viewed through the tectorial membrane and the first row of outer hair cell bundles at the right of the image.

significant structural changes as well as cellular intoxication owing to the mixing of endolymph and perilymph.

In 2005, Chan and Hudspeth developed a two-compartment experimental preparation that preserved the essential features of the cochlea (Chan and Hudspeth, 2005b, 2005a). However, they were unable to observe nonlinearities whose slopes closely matched those that characterize the active process in healthy cochleas. Building upon that work, we have now revisited and refined the protocol by implementing several critical improvements. By this means we are able to reliably measure in excised cochlear segments compressive nonlinearities comparable to those observed in intact cochleas.

2. Methods

All procedures involving animals were conducted following guidelines approved by the Institutional Animal Care and Use Committee of Rockefeller University. Mongolian gerbils of three to four weeks' age and of both sexes were euthanized by intraperitoneal injection of 200 $mg{\cdot}kg^{-1}$ pentobarbital sodium and phenytoin sodium (Euthasol®). The cochleas were excised and placed in a petri dish with dissecting solution containing 155 mM Na^{+}, 3 mM K^{+}, 250 μM Ca^{2+}, 1 mM Mg^{2+}, 154 mM Cl^{-}, 1 mM HPO^{2-}, 5 mM HEPES, 3 mM pyruvate, and 10 mM D (+)-glucose and with a pH of 7.3-7.4 and an osmolality of 310 $mOsm{\cdot}kg^{-1}$ [1]. We next transected the cochlea perpendicular to its helical axis, specifically between the basal and middle turns, and secured the isolated middle turn across a 1.5 mm hole in a plastic disc with isobutyl 2-cyanoacrylate (BOC Sciences). We then created optical access by opening windows in the thin bone layers that form the ceiling and floor of the middle cochlear turn and directly exposed the sensory epithelium of that turn. To prevent any leakage along the cochlear spiral, we sealed all openings of the cochlear duct with cyanoacrylate adhesive. We punctured Reissner's membrane and oriented the disc in a two-compartment acrylic recording chamber (Fig. 1). This entire procedure was generally accomplished within about 20 minutes. The basal surface of the cochlear segment was immersed in artificial perilymph that included the dissecting solution with the Ca^{2+} concentration enhanced to 2 mM. The apical surface was exposed to artificial endolymph that contained 150 mM KCl, 25 μM $CaCl_2$, 3 mM sodium pyruvate, 10 mM D-glucose, 5 mM HEPES, and 5 mM HPO^{2-} at a pH of 7.35. To ensure that the cochlear segment was continuously bathed in physiological solutions, the disc was placed between a pair of porous quartz frits (QPD10–4, Technical Glass Products). The hydrophilic nature of the frits ensured that each side of the preparation retained a thin layer of the appropriate solution. Silicone rubber gaskets helped form a tight seal between each compartment and the disc. We maintained all experimental solutions in an oxygenated state and utilized them at a consistent room temperature of 20-24 °C.

After signal conditioning in a unity-gain power amplifier (SA1, Tucker-Davis Technologies), acoustic stimuli were delivered to the lower compartment through high-performance speakers (Etymotic Research, ER-3C). The sound pressure was calibrated with a free-field microphone (4939-A-011, Brüel & Kjær). A pair of Ag/AgCl electrodes provided a steady endocochlear potential of 90-100 mV between the upper compartment and the lower one. A second pair of Ag/AgCl electrodes adjacent to the cochlear partition acquired cochlear-microphonic potentials in response to stimulation. The signal was amplified X100 by a DC differential amplifier (3000, A-M Systems) with low-pass filtering at 10 kHz, then amplified X200 and low-pass filtered at 5 kHz with an eight-pole Bessel filter (BM8.07, Kemo) before analog-to-digital conversion (PCIe-6353, National Instruments). All stimuli were synthesized and all responses were acquired with custom-written programs (LabVIEW 2019, National Instruments) at a sampling interval of 10 μs. In each experiment the noise floor from the microphonic signal was estimated as three times the standard deviation of the microphonic potential's amplitude in five consecutive frequency bins 1000 Hz distant from the stimulus frequency. Responses below the noise floor were rejected from the analysis.

In our preparation, the cochlear partition and its mounting disk exhibited a capacitance of approximately 33 pF, whereas the transepithelial resistance ranged from 5 to 50 kΩ. This yields an RC time constant of 0.2–1.7 μs, which is too short to allow effective temporal integration of asymmetrical transduction currents. As a result, we did not observe any summating potential under our experimental conditions.

To quantify the average slope of the nonlinear (sublinear) regime in cochlear microphonic responses as a function of sound pressure, each dataset was partitioned into two segments by systematically testing all possible split points. The lower-amplitude segment, exhibiting sublinear behavior, was distinguished from the higher-amplitude segment, which approximated a linear relationship in log–log coordinates. For each candidate partition, linear regressions were independently performed on both segments, yielding corresponding slopes and standard errors. The optimal split was defined as the point minimizing the combined standard errors from both regressions, thereby identifying the inflection point at which the data transitions between regimes. The inflection amplitude was then determined as the original amplitude value corresponding to this split, and the slope of the sublinear regime was subsequently calculated by linear regression in log–log space.

3. Results

3.1. Compressive nonlinearity in excised cochlear segments

At the beginning of each experiment, the range of characteristic frequencies represented in an excised cochlear segment was determined by delivering a calibrated chirp, or frequency sweep, covering 500-4000 Hz and recording the cochlear microphonic (CM) response. The resulting signals typically displayed a low-frequency peak centered near 1 kHz—possibly the result of a resonance in the apparatus—and a plateau between 2 kHz and 3 kHz (Fig. 2A). This range of frequencies coincides with the characteristic frequencies expected from the location of the exposed cochlear segment (Hutson et al., 2021).

When stimulated at a frequency within this range, a representative cochlear segment showed characteristic frequencies ranging from 2 kHz to 3 kHz and displayed behaviors similar to those observed in an intact, healthy cochlea (Ruggero et al., 1997; Robles and Ruggero, 2001). In particular, the microphonic responses to single-tone acoustic stimuli at a frequency f_{stim} = 2.66 kHz grew sublinearly as a function of the sound-pressure level (Fig. 2B). At low levels, the magnitude of the response increased with a doubly logarithmic slope of approximately 1/3. As the sound-pressure level rose, this growth transitioned to a linear regime. Notice that the sound-pressures in our experiments cannot be compared directly to those reported in studies *in vivo*, which benefit from the mechanical gain of the middle ear.

The transition was more obvious in plots of the segment's sensitivity, defined as the amplitude of the microphonic response relative to the sound pressure (Fig. 2C). In these terms and on doubly logarithmic coordinates, the nonlinear response decreased with a slope of approximately -2/3 with increasing sound pressure levels, then settled on a null slope after the response of the segment had become proportional to the intensity of the stimulus. Additional examples of compressive nonlinearities with a 1/3 power-law slope were measured from other cochlear segments (Fig. 3A). To quantify this compressive nonlinearity, we applied an iterative regime-splitting analysis in which each dataset was systematically partitioned into low-amplitude (sublinear) and high-amplitude (linear) segments, and linear regressions were performed in log–log space. This approach revealed that, on average, the nonlinear regime exhibited a slope of 0.34 ± 0.08 (mean ± SEM, n = 6)—consistent with the 1/3 power-law scaling characteristic of a Hopf bifurcation (Fig. 3A). As expected if the active process draws energy from the mechanoelectrical-transduction process of hair cells, and in keeping with observations both *in vivo* (Ruggero and Rich, 1991) and *ex*

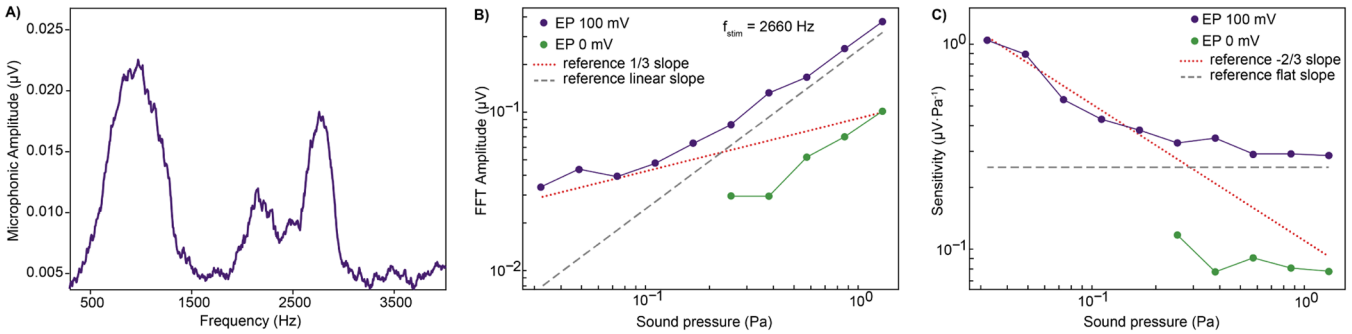

Fig. 2. Tuning and compressive nonlinearity in an isolated cochlear segment. (A) In the microphonic response as a function of frequency for a 200 ms frequency-sweep stimulus of 500-3000 Hz, the peak near 1000 Hz is suggestive of a resonance within the experimental apparatus. The peaks observed at higher frequencies bracket a plateau that includes the characteristic frequencies of the sensory hair cells under investigation. (B) A level function portrays the response of the same cochlear segment to a single tone at 2660 Hz with the artificial endocochlear potential set at 100 mV (violet circles). The amplitude of the cochlear microphonic voltage increases sublinearly for low stimulus pressures, transitioning to a linear increase at higher levels. In the absence of an endocochlear potential (green circles), the microphonic response diminishes and the signal emerges from the noise floor in a linear fashion. In these doubly logarithmic plots, a dashed gray line indicating linear growth and a dotted red line representing a slope of 1/3 have been included for reference. (C) When the same data are plotted in terms of sensitivity, the lines instead represent a null and a -2/3 slope.

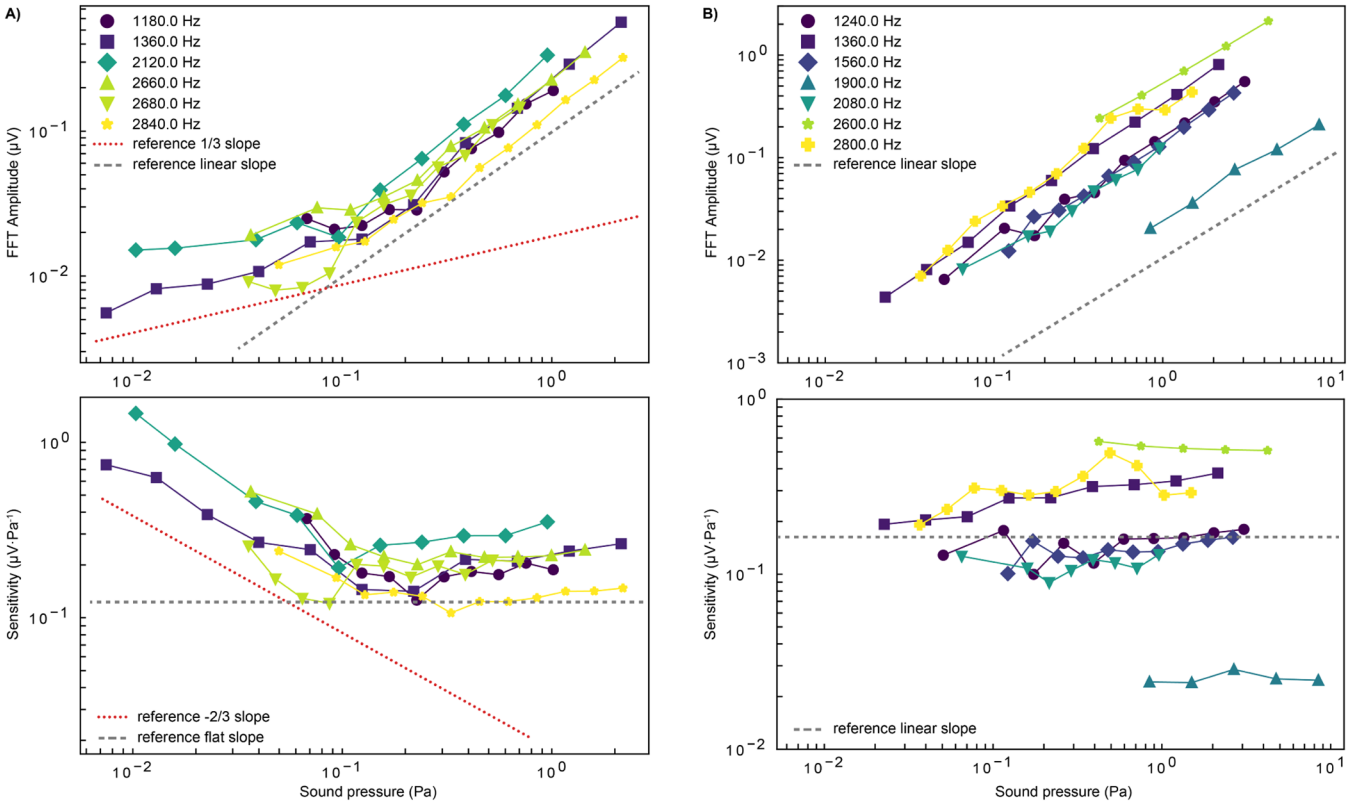

Fig. 3. Level functions and corresponding sensitivity plots for different cochlear segments. The top panels depict level functions (FFT amplitudes *versus* sound pressure) measured from different cochlear segments at various frequencies. (A) In a healthy preparation subjected to an artificial endocochlear potential of 100 mV and stimulated at its characteristic frequency, the cochlear microphonic (top panel) exhibits nonlinear growth. Nonlinear growth is represented by a red dotted line with a slope of 1/3, whereas linear growth is indicated by a gray dashed line. In the corresponding plots of sensitivity (lower panel), a red dotted line represents a −2/3 slope whereas a gray dashed line indicates a flat slope. The average slope for the nonlinear regime is 0.34 ± 0.08, the average slope of the linear regime is 1.09 ± 0.02. (B) Under other circumstances—in the absence of an endocochlear potential or when stimulated away from the segment's characteristic frequency—the microphonic response (top panel) and sensitivity (lower panel) both show predominantly linear growth.

vivo (Jacob et al., 2011), the nonlinearity was contingent upon the presence of an imposed endocochlear potential (Fig. 2B, and C).

In damaged or hypoxic preparations, in the absence of an artificial endocochlear potential, or during stimulation away from the segment's characteristic frequency, the response showed predominantly linear growth (Fig. 3B).

3.2. *Effect of pressure differences across the cochlear partition*

We observed that cochlear segments, when positioned with the perilymph compartment facing upward and the hair bundles pointed downward toward the sound source, exhibited more consistent compressive nonlinearities than preparations in the opposite orientation. We speculated that this effect resulted from the mechanical offset

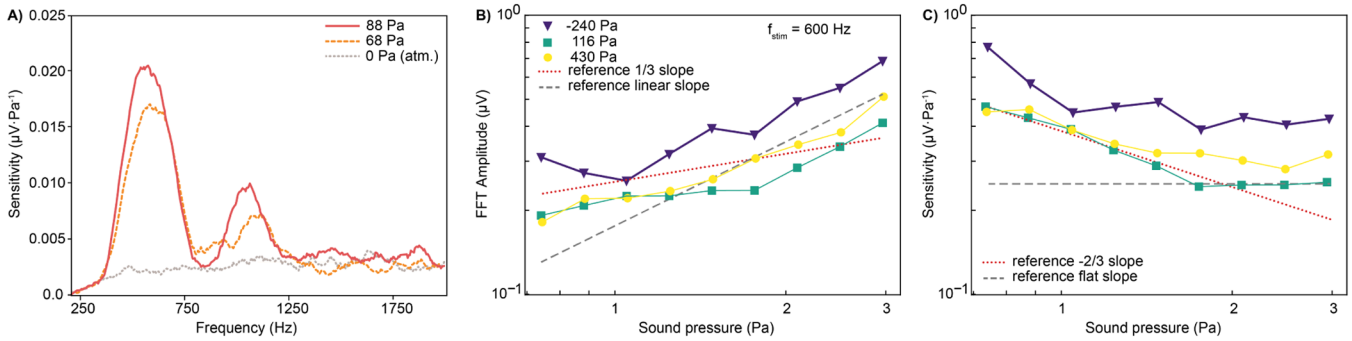

Fig. 4. The effect of static pressure on the microphonic response. (A) In the absence of a pressure difference across the cochlear partition—here mounted with the endolymphatic surface uppermost—the response to a frequency sweep of 300-3000 Hz displayed no peaks (dotted gray line). However, as the pressure in the lower compartment increased (dashed orange and continuous red lines), peaks emerged at approximately 550 Hz and 1050 Hz. (B) In a different preparation, a cochlear segment was also mounted with the endolymphatic surface uppermost but the exposed sensory epithelium was located >180° more apically along the tonotopic axis with respect to the segment in panel A. In this case the plots of level functions in response to sweep stimuli at the characteristic frequency of 600 Hz reveal the effects of larger positive and negative pressure biases in the lower compartment. A positive pressure of 116 Pa in the lower compartment (biasing the sensory epithelium towards the reticular lamina), reveals a compressive nonlinearity with a slope of about 1/3. A larger positive pressure in the lower compartment or a negative bias (biasing the sensory epithelium towards the basilar membrane) instead revealed more linear responses while having a relatively little effect on the magnitude of the cochlear microphonics. (C) The corresponding sensitivity curves reveal a slope of -2/3 at low levels of stimulation and a slope of zero (linear responsiveness) at high levels.

of the cochlear partition caused by the mass of saline solution weighing upon the preparation (Fridberger et al., 1997).

To test this hypothesis, we modified the apparatus to impose static pressures in the lower compartment to counteract the load on the cochlear partition. A manifold featuring three inlets and one outlet was connected to the pressure-speaker port of the lower compartment (Fig. 1). One of the inlets was connected to the speaker's output tube. Because the stimulus speaker was internally vented to atmospheric pressure, we wrapped its casing with thermoplastic film (Parafilm™) to prevent pressure leakage. A U-tube system partially filled with water was connected to the second inlet. By adding or subtracting controlled amounts of water at the opposite, open end, we imposed controlled static pressures. A digital manometer was connected to the remaining inlet to indicate the static pressure between stimuli.

While recording the cochlear microphonic responses with a frequency sweep of 300-3000 Hz, we progressively increased the pressure in the lower compartment. In the absence of any imposed pressure difference, the preparation did not exhibit frequency tuning (Fig. 4A). As we gradually increased the pressure in the lower compartment, the cochlear microphonic responses began to display two distinct peaks, the magnitude of which depended on the pressure difference.

In another experiment in which we exposed a segment centered near the apical end of the second turn, we applied a series of sweeps at different sound-pressure levels. At each pressure level, we mapped the level function at the peak frequency (Fig. 4B, and C). We observed that there was an optimal pressure at which the microphonic responses showed clear compression.

4. Discussion

The two-compartment cochlear preparation developed earlier by Chan and Hudspeth (Chan and Hudspeth, 2005a, 2005b), has been analyzed in detail (Nankali and Grosh, 2017) and has proven useful for experiments by other research groups (Jabeen et al., 2020). We have now enhanced the approach to establish *ex vivo* the conditions necessary to measure compressive nonlinearities that closely resemble those observed in intact cochleae. In particular, we optimized the dissection protocol and improved the chemical composition of the physiological solutions by transitioning to HEPES-based saline solutions, which supplanted phosphate buffers. This decision was predicated on two considerations. First, phosphate buffers' multiple protonation states and pH-dependent equilibria introduce uncertainties in the estimation of the free Ca^{2+} concentration (Recillas et al., 2012). Second, after long experiments we noted a pinkish-white substance that corresponded to the calcium phosphate precipitate that formed at elevated pH levels subsequent to the loss of chloride from an electrode (Lei et al., 2017). This substance gradually accumulated on the negative perilymphatic electrode used to sustain the endocochlear potential. This problem was absent with HEPES-based solutions.

We additionally determined the importance of the static pressure difference across the cochlear segment for the emergence of a compressive nonlinearity. As the pressure difference changed, it is highly likely that the resting position of the cochlear partition was also altered. This in turn influenced the resting state of the mechanosensitive ion channels, whose opening and closing underlie all models of the cochlear active process.

A 10 mm column of solution in the upper compartment is expected to exert a hydrostatic pressure of about 99 Pa on the cochlear partition. Given an opening area $A = 500\ \mu m \times 70\ \mu m = 3.5{\cdot}10^{-8}\ m^2$, this pressure represents a total force of 3.46 μN. Considering a point stiffness near 120 $N{\cdot}m^{-1}$ for the cochlear partition (Chan and Hudspeth, 2005a), we estimate that the hydrostatic pressure displaces the partition by approximately 15 nm on average, enough to significantly alter the open probability of mechanosensitive ion channels in the mammalian cochlea (Beurg et al., 2010; Jacob et al., 2011). Because this estimate does not take into account the variability in area of the exposed cochlear partition and the effect that factor might have on the areal stiffness, it is challenging to determine the physiological resting position of the cochlear partition.

Given this complexity, developing an experimental system that minimizes or eliminates these biases would be highly beneficial. A chamber with a vertically oriented specimen, for example, could reduce gravitational effects that alter the natural resting position of cochlear components and thus foster a more accurate simulacrum of *in vivo* conditions.

In our experiments, a sublinear growth of the cochlear microphonic responses emerged directly from the noise floor as stimulus intensity increased, followed by a linear regime at higher intensities. In living cochleas (Ruggero et al., 1997; Overstreet et al., 2002; Chen et al., 2011), as well as in individual hair bundles in the bullfrog (Martin and Hudspeth, 2001), however, a linear regime is also often observed at lower stimulus intensities. Within the Hopf framework, this initial linear slope emerges from the fact that biological systems exhibit inherent stochastic fluctuations, *i.e.* they are noisy. A dynamical system poised

near a Hopf bifurcation, in the absence of noise, indeed transitions sharply from no response to sublinear growth. The introduction of random fluctuations (*e.g.* thermal noise or stochastic gating of the channels), however, introduces stochastic forcing that smears the critical transition, disrupts phase coherence, and imparts a nonzero complex impedance even at the bifurcation (Nadrowski et al., 2004; Dinis et al., 2012). In other words, random fluctuations effectively detune the dynamical system for low intensity stimuli and thus cause it to behave like a dynamical system below criticality, for which the response grows linearly (Dinis et al., 2012; Martin and Hudspeth, 2021). In living cochleas or in studies of individual hair bundles in the bullfrog, the noise level is often sufficient to reveal this linear domain at low amplitudes. In our *ex vivo* recordings, however, the instrumental noise floor likely exceeds the response amplitudes evoked by low-intensity stimuli, thereby masking the regime in which linear behavior would be expected.

Our improved two-compartment cochlear preparation demonstrates that critical hallmarks of the cochlear active process—most notably compressive nonlinearity—can be reliably preserved *ex vivo* through meticulous control of physiological conditions. Achieving this required refining dissection protocols to minimize exposed sensory tissue, precisely tuning ionic solutions to maintain calcium homeostasis, stabilizing the temperature of the sensory epithelium, and adjusting the transepithelial static pressure. That the resulting compressive nonlinearities align closely with expectations for a system operating near a Hopf bifurcation supports the hypothesis that critical dynamical behavior underlies the remarkable sensitivity and frequency selectivity observed in mammalian hearing. Further refinement of this approach—especially by minimizing the pressure biases on the sensory epithelium, which we demonstrate here to be significant—holds the promise of enabling more precise measurements and a deeper understanding of cochlear function under physiological conditions.

CRediT authorship contribution statement

Francesco Gianoli: Writing – review & editing, Writing – original draft, Visualization, Validation, Methodology, Investigation, Formal analysis, Data curation. **Rodrigo Alonso:** Writing – review & editing, Writing – original draft, Visualization, Validation, Methodology, Investigation, Formal analysis, Data curation. **Brian Fabella:** Validation, Methodology, Investigation. **A.J. Hudspeth:** Writing – review & editing, Writing – original draft, Resources, Project administration, Investigation, Funding acquisition, Conceptualization.

Data availability

Data will be made available on request.

References

Ashmore, J.F., 1987. A fast motile response in guinea-pig outer hair cells: the cellular basis of the cochlear amplifier. J. Physiol. 388, 323–347.

Beurg, M., Nam, J.-H., Chen, Q., Fettiplace, R., 2010. Calcium balance and mechanotransduction in rat cochlear hair cells. J. Neurophysiol. 104, 18–34.

Chan, D.K., Hudspeth, A.J., 2005a. Ca2+ current-driven nonlinear amplification by the mammalian cochlea *in vitro*. Nat. Neurosci. 8, 149–155.

Chan, D.K., Hudspeth, A.J., 2005b. Mechanical responses of the organ of corti to acoustic and electrical stimulation *in vitro*. Biophys. J. 89, 4382–4395.

Chen, F., Zha, D., Fridberger, A., Zheng, J., Choudhury, N., Jacques, S.L., Wang, R.K., Shi, X., Nuttall, A.L., 2011. A differentially amplified motion in the ear for near-threshold sound detection. Nat. Neurosci. 14, 770–774.

Dallos, P., 2008. Cochlear amplification, outer hair cells and prestin. Curr. Opin. Neurobiol. 18, 370–376.

Dinis, L., Martin, P., Barral, J., Prost, J., Joanny, J.F., 2012. Fluctuation-response theorem for the active noisy oscillator of the hair-cell bundle. Phys. Rev. Lett. 109, 160602.

Fridberger, A., van Maarseveen, J.T., Scarfone, E., Ulfendahl, M., Flock, B., Flock, A., 1997. Pressure-induced basilar membrane position shifts and the stimulus-evoked potentials in the low-frequency region of the guinea pig cochlea. Acta Physiol. Scand. 161, 239–252.

Hudspeth, A.J., 2008. Making an effort to listen: mechanical amplification in the ear. Neuron 59, 530–545.

Hudspeth, A.J., 2014. Integrating the active process of hair cells with cochlear function. Nat. Rev. Neurosci. 15, 600–614.

Hudspeth, A.J., Jülicher, F., Martin, P., 2010. A critique of the critical cochlea: hopf–a bifurcation–is better than none. J. Neurophysiol. 104, 1219–1229.

Hudspeth, A.J., Martin, P., 2024. The critical thing about the ear's sensory hair cells. J. Neurosci. 44, e1583242024.

Hutson, K.A., Pulver, S.H., Ariel, P., Naso, C., Fitzpatrick, D.C., 2021. Light sheet microscopy of the gerbil cochlea. J. Comp. Neurol. 529, 757–785.

Jabeen, T., Holt, J.C., Becker, J.R., Nam, J.-H., 2020. Interactions between passive and active vibrations in the organ of corti *In vitro*. Biophys. J. 119, 314–325.

Jacob, S., Pienkowski, M., Fridberger, A., 2011. The endocochlear potential alters Cochlear micromechanics. Biophys. J. 100, 2586–2594.

Lei, Y., Song, B., van der Weijden, R.D., Saakes, M., Buisman, C.J.N., 2017. Electrochemical induced calcium phosphate precipitation: importance of local pH. Environ. Sci. Technol. 51, 11156–11164.

Martin, P., Hudspeth, A.J., 1999. Active hair-bundle movements can amplify a hair cell's response to oscillatory mechanical stimuli. Proc. Natl. Acad. Sci. USA 96, 14306–14311.

Martin, P., Hudspeth, A.J., 2001. Compressive nonlinearity in the hair bundle's active response to mechanical stimulation. Proc. Natl. Acad. Sci. USA 98, 14386–14391.

Martin, P., Hudspeth, A.J., 2021. Mechanical frequency tuning by sensory hair cells, the receptors and amplifiers of the inner ear. Annu. Rev. Condens. Matter Phys. 12, 29–49.

Nadrowski, B., Martin, P., Jülicher, F., 2004. Active hair-bundle motility harnesses noise to operate near an optimum of mechanosensitivity. Proc. Natl. Acad. Sci. USA 101, 12195–12200.

Nankali, A., Grosh, K., 2017. Simulating the Chan-Hudspeth experiment on an active excised cochlear segment. J. Acoust. Soc. Am. 142, 215–227.

Overstreet 3rd, E.H., Temchin, A.N., Ruggero, M.A., 2002. Basilar membrane vibrations near the round window of the gerbil cochlea. J Assoc Res Otolaryngol JARO 3, 351–361.

Pickles, J.O., 2012. An introduction to the physiology of hearing, 4. Emerald, London.

Recillas, S., Rodríguez-Lugo, V., Montero, M.L., Viquez-Cano, S., Hernandez, L., Castano, V.M., 2012. Studies on the precipitation behaviour of calcium phosphate solutions. J Ceram Process Res 13, 5–10.

Robles, L., Ruggero, M.A., 2001. Mechanics of the mammalian Cochlea. Physiol. Rev. 81, 1305–1352.

Ruggero, M.A., Rich, N.C., 1991. Furosemide alters organ of corti mechanics: evidence for feedback of outer hair cells upon the basilar membrane. J. Neurosci. 11, 1057–1067.

Ruggero, M.A., Rich, N.C., Recio, A., Narayan, S.S., Robles, L., 1997. Basilar-membrane responses to tones at the base of the chinchilla cochlea. J. Acoust. Soc. Am. 101, 2151–2163.

Strogatz, S.H., 1994. Nonlinear Dynamics and Chaos: With Applications to Physics, Biology, Chemistry, and Engineering. Addison-Wesley Pub, Reading, Mass.